LUND UNIVERSITY

The effects of counterion exchange on charge stabilization for anionic surfactants in nonpolar solvents

Smith, Gregory N.; Brown, Paul; James, Craig; Kemp, Roger; Muhammad Khan, Asad; Plivelic, Tomás; Rogers, Sarah E.; Eastoe, Julian

Published in:
Journal of Colloid and Interface Science

DOI:
10.1016/j.jcis.2015.11.062

2016

Link to publication

Citation for published version (APA):
Smith, G. N., Brown, P., James, C., Kemp, R., Muhammad Khan, A., Plivelic, T., Rogers, S. E., & Eastoe, J. (2016). The effects of counterion exchange on charge stabilization for anionic surfactants in nonpolar solvents. *Journal of Colloid and Interface Science*, *465*, 316-322. https://doi.org/10.1016/j.jcis.2015.11.062

Total number of authors:
8

General rights
Unless other specific re-use rights are stated the following general rights apply:
Copyright and moral rights for the publications made accessible in the public portal are retained by the authors and/or other copyright owners and it is a condition of accessing publications that users recognise and abide by the legal requirements associated with these rights.
• Users may download and print one copy of any publication from the public portal for the purpose of private study or research.
• You may not further distribute the material or use it for any profit-making activity or commercial gain
• You may freely distribute the URL identifying the publication in the public portal

Read more about Creative commons licenses: https://creativecommons.org/licenses/

Take down policy
If you believe that this document breaches copyright please contact us providing details, and we will remove access to the work immediately and investigate your claim.

LUND UNIVERSITY

PO Box 117
221 00 Lund
+46 46-222 00 00

Supporting Information—The effects of counterion exchange on charge stabilization for anionic surfactants in nonpolar solvents

Gregory N. Smith[a,1,*], Paul Brown[a,2], Craig James[a,3], Roger Kemp[b,4], Asad Muhammad Khan[a,5], Tomás S. Plivelic[c], Sarah E. Rogers[d], Julian Eastoe[a,**]

[a]*School of Chemistry, University of Bristol, Cantock's Close, Bristol, BS8 1TS, United Kingdom*
[b]*Merck Chemicals Ltd, University Parkway, Chilworth, Southampton, SO16 7QD, United Kingdom*
[c]*MAX IV Laboratory, Lund University, Box 118, SE-221 00 Lund, Sweden*
[d]*ISIS-STFC, Rutherford Appleton Laboratory, Chilton, Oxon OX11 0QX, United Kingdom*

S1. Materials

S1.1. Acid-base neutralization.

A 1 wt % solution of NaAOT was prepared in water and run through a column containing Amberlite IR120 hydrogen form to obtain the acid form of AOT in a 1 L round bottom flask. This material was not isolated, and it was immediately neutralized with a solution of metal hydroxide in water. The hydroxides were used as provided: lithium hydroxide monohydrate ($\geq$ 99.0%, Sigma–Aldrich), potassium hydroxide (99% trace metals basis, semiconductor grade, Sigma–Aldrich), and rubidium hydroxide solution (50 wt % solution in H_2O, 99.9% trace metals basis, Aldrich). The pH was monitored, and the base solution added to neutralization. The water was carefully evaporated to avoid bumping.

S1.2. Metathesis.

A 0.1 M solution (150 mL) of NaAOT in ethanol was combined with a 1 M solution (300 mL) of cesium chloride (> 99%, BDH) in water in a separating funnel. The resulting polar solvent solution was clear. Diethyl ether (50 mL) was added to the separating funnel, and the extraction left overnight. The organic phase containing the CsAOT was isolated, and the solvent evaporated.

S1.3. Surfactant purity

LiAOT (Calc. for $C_{20}H_{37}LiO_7S$: C, 56.1%; H, 8.7%; S, 7.5%. Found: C, 56.0%; H, 8.6%; S, 5.1%; Na, 0.0%.); NaAOT (^{1}H NMR (300 MHz, $CDCl_3$) 0.87 (12 H), 1.27 (16 H), 1.54 (2 H), 3.19 (1 H), 4.02 (4 H), 4.34 (2 H). Calc. for $C_{20}H_{37}NaO_7S$: C, 54.0%; H, 8.4%; Na, 5.2%; S, 7.2%. Found: C, 54.0%; H, 8.3%; Na, 4.9%; S, 7.0%.); KAOT (Calc. for $C_{20}H_{37}KO_7S$: C, 52.2%; H, 8.1%; S, 7.0%. Found: C, 52.4%; H, 8.1%; S, 3.8%; Na, 0.0%.); RbAOT (Calc. for $C_{20}H_{37}RbO_7S$: C, 47.4%; H, 7.4%; S, 6.3%. Found: C, 46.6%; H, 7.2%; S, 3.7%; Na, 0.0%.); CsAOT (Calc. for $C_{20}H_{37}CsO_7S$: C, 43.3%; H, 6.7%; S, 5.8%. Found: C, 43.3%; H, 6.7%; S, 4.0%, Na, 0.0%; Cl, 0.0%.)

*Corresponding author
**Principal corresponding author
Email addresses: g.n.smith@sheffield.ac.uk (Gregory N. Smith), julian.eastoe@bristol.ac.uk (Julian Eastoe)
[1]Current address: Department of Chemistry, University of Sheffield, Brook Hill, Sheffield, South Yorkshire, S3 7HF, United Kingdom
[2]Current address: Department of Chemical Engineering, Massachusetts Institute of Technology, Cambridge, Massachusetts 02139, United States of America
[3]Current address: Department of Chemistry and CSGI, University of Florence, 50019 Sesto Fiorentino, Firenze, Italy
[4]Current address: Battelle UK, Hampshire, PO9 1SA, United Kingdom
[5]Current address: COMSATS Institute of Information Technology, Abbottabad, Pakistan

S1.4. PMMA latexes

MC1 and MC2 latexes were a gift from Merck Chemicals Ltd. and were prepared using the method described by Antl *et al* [1]. MC2 latexes also included a magenta dye that was added during polymerization. The Z-average solvodynamic diameter of MC1 in dodecane was 412 ± 5 nm with a polydispersity index of 0.07 (Malvern ZetaSizer Nano S90). The solvodynamic diameter of MC2 in dodecane was 438 nm with a polydispersity index of 0.01 (Brookhaven ZetaPlus).

S2. Methods

S2.1. Sans2d (ISIS)

A simultaneous Q-range of 0.004–0.80 Å^{-1} was achieved utilizing an incident wavelength range of 1.75–16.5 Å and employing an instrument set up of L_1=L_2=4 m, with the 1 m^2 detector offset vertically 150 mm and sideways 269 mm. The beam diameter was 12 mm. On LOQ, data were recorded on a single two-dimensional detector to provide a simultaneous Q-range of 0.008–0.24 Å^{-1} utilizing neutrons with $2 \leq \lambda \leq 10$ Å. The beam diameter was 8 mm.

Data have been fit to models as described in the text using the SasView small-angle scattering software package [2]. Form factors ($P(Q)$) for spheres [3, 4] and ellipsoids [5, 6] were used depending on the system being studied. The distribution of particle size has been accounted for using the Schulz distribution [7].

S2.2. I911-SAXS (Max IV Laboratory)

Samples were measured in a 1.5 mm diameter quartz capillary in a flow-through cell to ensure that the cell geometry was equivalent for solvent and sample measurements. Data were recorded on a two-dimensional hybrid pixel array X-ray detecctor (PILATUS 1M, Dectris). A Q-range of 0.016–0.76 Å^{-1} was achieved using an X-ray wavelength of 0.91 Å and a sample-detector distance of 1.4 m. Data were radially integrated using YAX 2.0, a macro script for ImageJ [8, 9]. Data have been fit to a spherical form factor [3, 4] using the SasView small-angle scattering analysis software package [2]. The distribution of particle size has been accounted for using the Schulz distribution [7]. The fitting was weighted by $|\sqrt{I(Q)}|$.

S3. Small-angle scattering data fitting

The best fit parameters to SANS and SAXS data are shown in the following tables. Experimental SANS curves for MAOT surfactants in dodecane-d_{26} are shown in Figure S1. The sphere radius (r) and the width of the Schulz distribution (σ_{Sch}) are shown. For CsAOT in dodecane-d_{26}, the scattering curve is fit to an ellipsoidal form factor with r_p as the polar radius and r_e as the equatorial radius. The scale factor for SANS measurements is equivalent to the volume fraction of inverse micelles in the solution as the scattering length densities for surfactant and solvent are fixed.

Porod analysis was also performed on the SANS measurements of MAOT surfactants in cyclohexane-d_{12}. At high-Q, the total scattering ($I(Q)$) is sensitive to local interfaces and can be related to the specific surface area (Σ) through the Porod law, Equation S1 [10] .

$$\lim_{Q \to \infty} I(Q) = 2\pi\Delta\rho^2\Sigma Q^{-4} \tag{S1}$$

By determining the asymptote in the limit of high-Q (practically for AOT inverse micelles at $Q > 0.1$ Å^{-1}) and assuming strong binding, it is possible to estimate the surface area of each surfactant molecule at the inverse micelle interface [11]. Porod plots are shown in Figure S2 and calculated areas per molecule (a_s) are shown in Table S1.

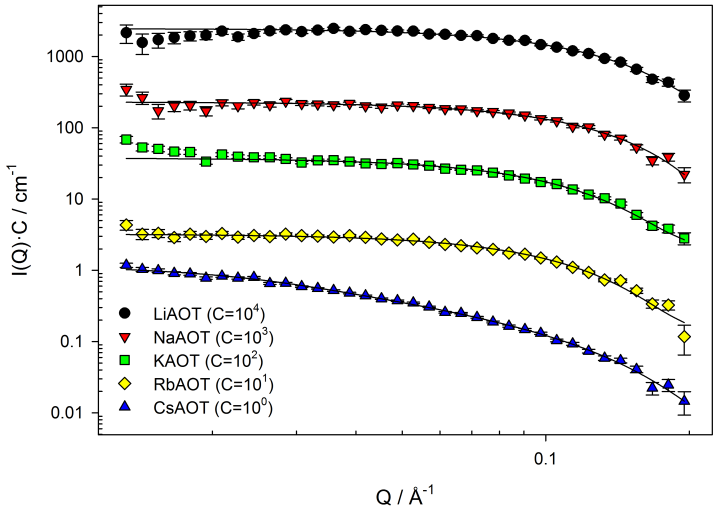

Figure S1: SANS curves for MAOT surfactants in dodecane-d_{26}. The droplets (CsAOT excluded) have radii between 16 and 20 Å. CsAOT droplets are well fit as ellipsoids with a sphere equivalent radius of 30 Å.

Table S1: SANS and SAXS data fitting parameters for MAOT inverse micelles in cyclohexane.

SANS in cyclohexane-d_{12} Surfactant	Fit scale / 10^{-3}	r / ±1 Å	σ_{Sch}	$a_s \pm 1$ / Å^2
LiAOT	2.68	15.3	—	215
NaAOT[a]	3.34	15.6	—	217
KAOT	2.91	16.6	—	198
RbAOT	2.72	17.4	—	176
CsAOT	3.51	12.9	0.26	182

[a] Previously measured (Smith *et al.* [12])

SAXS in cyclohexane Surfactant	r / ±1 Å	σ_{Sch}
LiAOT	10.0	0.07
NaAOT	10.8	0.13
KAOT	10.0	0.12
RbAOT	10.0	0.15
CsAOT	9.6	0.20

Table S2: SANS data fitting parameters for MAOT inverse micelles in dodecane-d_{26}.

Surfactant	Fit scale /10^{-3}	r / ±1 Å
LiAOT	3.37	16.4
NaAOT	3.21	16.6
KAOT	2.86	20.0
RbAOT	2.41	20.1
CsAOT[a]	1.81	29.9

[a] Fit to ellipsoidal form factor with $r_p = 112.7$ Å and $r_e = 15.4$ Å. r denotes the sphere equivalent radius.

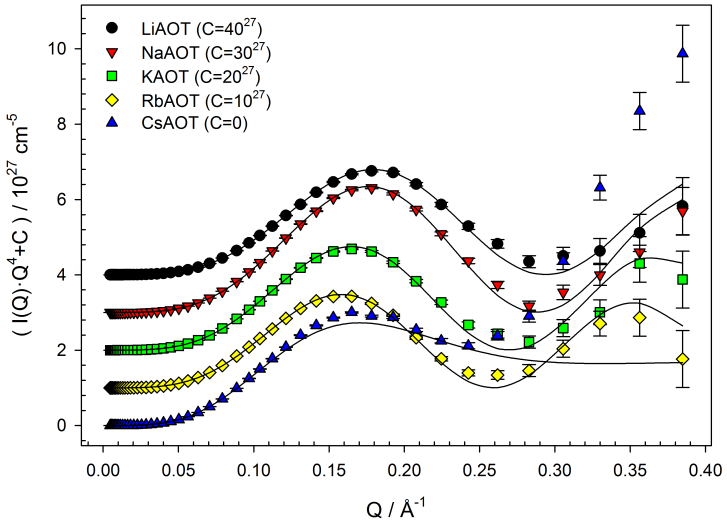

Figure S2: Porod plots ($I(Q) \cdot Q^4$ as a function of Q) for SANS measurements of MAOT surfactants in cyclohexane-d_{12}.

References

[1] L. Antl, J. W. Goodwin, R. D. Hill, R. H. Ottewill, S. M. Owens, S. Papworth, J. A. Waters, The preparation of poly(methyl methacrylate) latices in non-aqueous media, Colloids Surf. 17 (1) (1986) 67–78. doi:10.1016/0166-6622(86)80187-1.

[2] Sasview for small angle scattering analysis.
URL http://www.sasview.org/

[3] Lord Rayleigh, The incidence of light upon a transparent sphere of dimensions comparable with the wave-length, Proc. R. Soc. London A 84 (567) (1910) 25–46. doi:10.1098/rspa.1910.0054.

[4] A. Guinier, G. Fournet, Small-Angle Scattering of X-Rays, John Wiley & Sons, New York, 1955.

[5] A. Guinier, La diffraction dex rayons X aux très petits angles: Application à l'étude de phénomènes ultramicroscopiques, Ann. Phys. 12 (1939) 161–237.

[6] L. A. Feigin, D. I. Svergun, Structure Analysis by Small-Angle X-Ray and Neutron Scattering, Plenum Press, New York, 1987.

[7] G. V. Schulz, Z. Phys. Chem. Abt. B 43 (1939) 25–46.

[8] S. L. Gras, A. M. Squires, Dried and hydrated x-ray scattering analysis of amyloid fibrils, in: A. F. Hill, K. J. Barnham, S. P. Bottomley, R. Cappai (Eds.), Protein Folding, Misfolding, and Disease, Vol. 752 of Methods in Molecular Biology, Humana Press, 2011, pp. 147–163. doi:10.1007/978-1-60327-223-0_10.

[9] T. Snow, Yax 2.0.
URL http://www.cunninglemon.com/projects.YAX.html

[10] I. Grillo, Small-angle neutron scattering and applications in soft condensed matter, in: R. Borsali, R. Pecora (Eds.), Soft Matter Characterization, Springer Netherlands, 2008, pp. 723–782. doi:10.1007/978-1-4020-4465-6_13.

[11] J. Eastoe, T. F. Towey, B. H. Robinson, J. Williams, R. K. Heenan, Structures of metal bis(2-ethylhexylsulfosuccinate) aggregates in cyclohexane, J. Phys. Chem. 97 (7) (1993) 1459–1463. doi:10.1021/j100109a035.

[12] G. N. Smith, P. Brown, S. E. Rogers, J. Eastoe, Evidence for a critical micelle concentration of surfactants in hydrocarbon solvents, Langmuir 29 (10) (2013) 3252–3258. doi:10.1021/la400117s.